Interchain hydrogen-bonding interactions may facilitate translocation of K^+ ions across the potassium channel selectivity filter, as suggested by synthetic modeling chemistry

Juan C. Mareque Rivas, Harald Schwalbe, and Stephen J. Lippard*

Department of Chemistry, Massachusetts Institute of Technology, Cambridge, MA 02139

Contributed by Stephen J. Lippard, May 23, 2001

A 4-fold symmetric arrangement of TVGYG polypeptides forms the selectivity filter of the K^+ channel from *Streptomyces lividans* (KcsA). We report the synthesis and properties of synthetic models for the filter, *p-tert*-butyl-calix[4]arene-$(OCH_2CO\text{-}XOBz)_4$ (X = V, VG, VGY), 1–3. The first cation (Na^+, K^+) binds to the four -{OCH_2CO}- units, a region devised to mimic the metal-binding site formed by the four T residues in KcsA. NMR studies reveal that cations and valine amide protons compete for the carbonyl oxygen atoms, converting $N—H_{Val}\cdots O{=}C$ hydrogen bonds to $M^+\cdots O{=}C$ bonds (M^+ = Na^+ or K^+). The strength of these interchain $N—H_{Val}\cdots O{=}C$ hydrogen bonds varies in the order 3 > 2 > 1. We propose that such interchain H-bonding may destabilize metal binding in the selectivity filter and thus help create the low energy barrier needed for rapid cation translocation.

Potassium channels are integral membrane proteins that regulate the fast and selective movement of K^+ ions across the cell membrane (1). Recently, the landmark x-ray structure of the K^+ channel from *Streptomyces lividans* (KcsA) was reported (2). This structure revealed carbonyl oxygen atoms from four TVGYG sequences, residues 75 to 79, arranged in a 4-fold symmetric structure called the selectivity filter and positioned in a line to provide consecutive and closely spaced binding sites for the passing ions. From a coordination chemistry perspective, the rapid movement of K^+ ions at $\approx 10^6\ s^{-1}$ across the cell membrane is a succession of ion-binding and release events. The details of how this chemistry is achieved are not fully elucidated.

The x-ray structure of KcsA is consistent with the notion that interaction with main-chain carbonyl and T75 side-chain hydroxyl oxygens of four TVGYG units perfectly compensates for the loss of K^+-bound water molecules of the incoming hydrated K^+ ion. The pore is apparently constrained at a width sufficient to prevent favorable interactions with the smaller Na^+ ions, which retain some bound water and thus cannot pass through the filter. Such a difference could account at least in part for the K^+ selectivity of the channel. The role that the side chains of residues 75 to 79 play in defining the pore structure, and thus channel function, must be important given that the TVGYG sequence is almost universally conserved among K^+-selective channels and tolerates very few mutations (2, 3). In addition, theories about potassium ion permeation across K^+ channels postulate that destabilization of metal binding caused by repulsion between ions in a multiply ion-populated selectivity filter (2, 4–6) accounts for their rapid movement. The K_d for binding the first K^+ ion to T75, on the cytoplasmic side of the selectivity filter of KcsA, has not to our knowledge been determined. Nevertheless, it is reasonable to expect that its value will be smaller than that for binding at Y78, which is located on the extracellular side of the selectivity filter; with Ba^{2+} ions bound to T75, the latter K_d is $\approx 3\ \mu M$ (7).

The x-ray structure of KcsA is limited in resolution to only 3.2 Å, which prevents an accurate location of the main-chain atoms and cation occupancy along the selectivity filter. There is, moreover, much to be understood about K^+ channel gating (8) and ion permeation (9). Little is known about possible structural rearrangements that might modulate the nature and strength of ion binding as the K^+ ions pass through.

In the present report, we describe the first step in an approach to elucidate aspects of these issues through synthetic modeling chemistry and NMR spectroscopy. In particular, we have constructed a replica of a portion of the K^+ channel selectivity filter in which *p-tert*-butyl-calix[4]-$(OCH_2COOH)_4$ was used as the molecular template. This molecule was chosen because it binds monovalent ions in a fashion that reproduces geometrically (Fig. 1) the T75 K^+-binding site in KcsA. To compare the geometries, the coordinates of residues 75 to 79 of the x-ray structure of KcsA (2) were overlaid on the energy-minimized structure of *p-tert*-butyl-calix[4]-$(OCH_2COCl)_4$ by using the computer program INSIGHT II, revealing an excellent size match (Fig. 1 and Fig. 11, which is published as supplemental data on the PNAS web site, www.pnas.org). Metal binding at this site in calixarenes leads to characteristic proton NMR chemical shift changes, offering a powerful structural tool (10–14). Four VGY peptide sequences were attached, one amino acid at a time, to *p-tert*-butyl-calix[4]-$(OCH_2COOH)_4$ with the intention of creating a structural mimic of the region where cations are located in KcsA, namely, the TVGY portion of the selectivity filter. The binding of Na^+ and K^+ to *p-tert*-butyl-calix[4]-$(OCH_2CO\text{-}V\text{-}OBz)_4$ **1**, *p-tert*-butyl-calix[4]-$(OCH_2CO\text{-}V\text{-}G\text{-}OBz)_4$ **2**, and *p-tert*-butyl-calix[4]-$(OCH_2CO\text{-}V\text{-}G\text{-}Y\text{-}OBz)_4$ **3**, investigated by NMR and IR spectroscopy, is described here.

Materials and Methods

General. All compounds were prepared under Ar unless otherwise indicated. Solvents were dried and purified under N_2 by using standard methods and were distilled immediately before use. Starting materials were purchased from commercial sources and used without further purification. *p-tert*-Butyl-calix[4]arene tetraethyl ester was prepared by adaptation of a literature procedure (10) and hydrolyzed to the tetraacid under basic conditions. *p-tert*-Butyl-calix[4]arene tetraacid chloride was prepared from the tetraacid by reaction with excess (≈10-fold) oxalyl chloride in dichloromethane. NMR spectra were collected on Varian 500 MHz or Bruker 600 MHz (Billerica, MA) spectrometers. Chemical shifts were referenced with respect to the residual CH_3CN peak, δ 1.94 ppm. MS analyses were performed on a Finnigan-MAT (San Jose, CA) spectrometer

Abbreviations: KcsA, potassium channel of *Streptomyces lividans*; MALDI–TOF, matrix-assisted laser desorption ionization time of flight.

*To whom reprint requests should be addressed. E-mail: lippard@lippard.mit.edu.

The publication costs of this article were defrayed in part by page charge payment. This article must therefore be hereby marked "*advertisement*" in accordance with 18 U.S.C. §1734 solely to indicate this fact.

 www.pnas.org/cgi/doi/10.1073/pnas.161257798

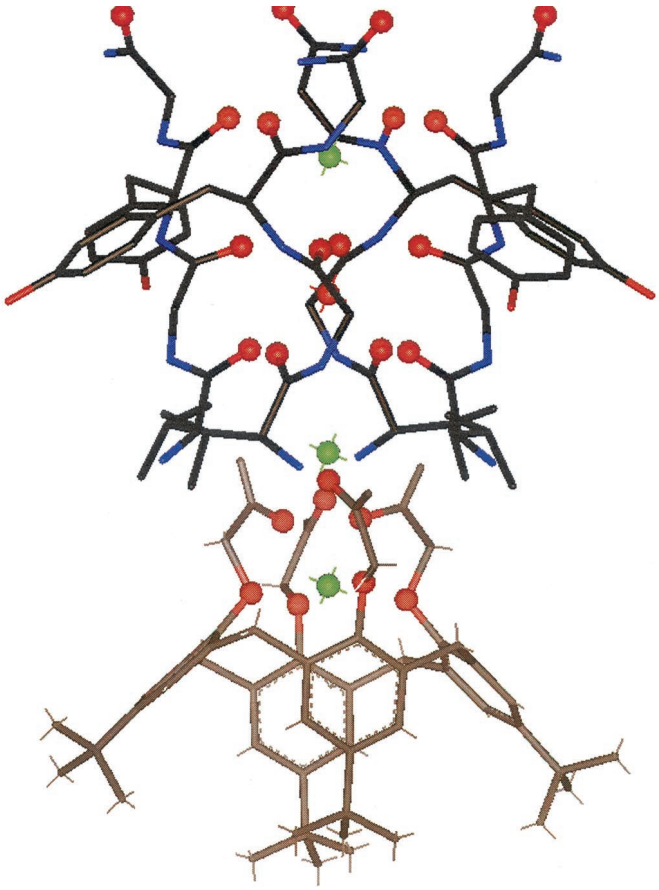

Fig. 1. View of the VGYG portion of the selectivity filter structure, drawn with coordinates from Doyle *et al.* (2), overlaid on that of *p-tert*-butyl-calix[4]arene-$(OCH_2COCl)_4$ showing how the four -{OCH_2CO}- calixarene units mimic the four T75 residues (see text). In some K^+ channels, T75 is replaced by a serine. Red, blue, and black colors designate oxygen, nitrogen, and carbon atoms, respectively. Ion and water locators (green and red) are assigned as in the x-ray structure, but we do not claim identical locations in our synthetic model compounds.

operated in the electrospray ionization mode or a PerSeptive Biosystems (Framingham, MA) Voyager matrix-assisted laser desorption ionization time-of-flight (MALDI-TOF) spectrometer. IR spectra were recorded on a Bio-Rad FTS-135 Fourier-transformed IR instrument. Molecular modeling was performed on a Silicon Graphics (Mountain View, CA) computer with the INSIGHT II computer program.

Synthesis. *p-tert-Butyl-calix[4]arene Tetra-valine Benzyl Ester* **1**. In a typical reaction, valine benzyl ester hydrochloride (2.3 g, 10 mmol) was suspended in dry CH_2Cl_2 (60 ml), after which *N*-methylmorpholine (4 ml, 40 mmol) was added to deprotonate and solubilize the amino acid. To this solution was added *p-tert*-butyl-calix[4]arene tetracarboxylic acid chloride (1.4 g, 1.5 mmol). The mixture was stirred at ambient temperature for 14 h. Then 1 N HCl (aq.) (30 ml) was added. The organic layer was separated and washed with water (2 × 20 ml), dried over $MgSO_4$, and evaporated under vacuum to give a yellowish solid. This solid was washed with 10 ml of acetone to give a pure (by TLC, NMR, and MS) white product (1.6 g, 66%). ^{1}H NMR ($CDCl_3$, 500 MHz, 293 K), δ (ppm) 7.28–7.34 [m, 12H, Ar(*Bz*)], 6.73 (s, 8H, Ar*H*), 4.68 and 3.17 (d, J = 13 Hz, 4H, 4H, ArCH_2Ar), 5.13 and 5.02 (d, J = 12.5 Hz, 4H, 4H, CH_2-Bz), 4.86 and 4.54 (s, J = 13.5, 4H, 4H, OCH_2CO), 4.6 (m, 4H, Val-C$_\alpha H$), 2.11 (m, J = 6.5 Hz, 4H, Val-C$_\beta H$), 1.07 [s, 36H, C(CH_3)$_3$], 0.77 and 0.81 [d, J = 6.5 Hz, 4H, 4H, Val-($C_\gamma H_3$)$_2$]. MALDI-TOF-MS (+ion, 2,5-dihydroxybenzoic acid): Found, 1637.59 (H^+), Calcd, 1637.91 (H^+); Found, 1659.2 (Na^+), Calcd, 1659. 89 (Na^+).

p-tert-*Butyl-calix[4]arene Tetra-valine-OH.* The calixarene tetravaline benzyl ester (1.6 g, 0.96 mmol) was added to a suspension of 10% Pd/C (0.1 g) in oxygen-free methanol (40 ml). The mixture was stirred at room temperature under a H_2 atmosphere for 26 h. The solution was filtered to remove the solids, and the filtrate was evaporated to afford the crude product. ^{1}H NMR ($CDCl_3$, 500 MHz, 293 K), δ (ppm) 6.68 (s, 8H, Ar*H*), 4.9 (br), 4.63 (br), 4.51 (br), 3.1 (br), 2.04 (br), 1.04 (s), 0.88–0.74 (br). Electrospray ionization-MS (-ion, MeOH/NEt_3): 1276.7. MALDI-TOF-MS (+ion, 2,5-dihydroxybenzoic acid): Found, 1277.76 (H^+) Calcd, 1277.72 (H^+); Found, 1299.30 (Na^+), Calcd, 1299.70 (Na^+).

p-tert-*Butyl-calix[4]arene Tetra-valine-glycine-Benzyl Ester* **2**. *N*-methylmorpholine (0.8 ml, 7.82 mmol) was added to a solution of glycine benzyl ester hydrochloride (1.57 g, 7.82 mmol) in dimethylformamide (1.6 ml). To this solution was then added *p-tert*-butyl-calix[4]arene tetravaline (0.5 g, 0.391 mmol) followed by *N*-hydroxybenzotriazole (HOBt) (1.06 g, 7.82 mmol). This mixture was stirred for 15 min, after which dicyclohexylcarbodiimide (1.62 g, 7.82 mmol) was added. The resulting mixture was protected from light and stirred at ambient temperature for 18 h. The solvent was evaporated and the viscous material partially redissolved in CH_2Cl_2 (30 ml). The solution was filtered and the filtrate washed with 2 N HCl (aq) (20 ml), followed by 5% $NaHCO_3$ (aq) (2 × 10 ml). The organic layer was separated and solvent evaporated. The thick viscous pale yellow material was washed with acetone (40 ml) to give a white solid (0.52 g, 71%). This crude material was purified by reversed-phase column chromatography by using C18 silica eluting first with CH_3CN/H_2O (7:1) and finishing with 100% MeOH. ^{1}H NMR ($CDCl_3$, 500 MHz, 293 K), δ (ppm) 8.1 (br, 4H, Gly-N*H*), 6.71 (br, 4H, Val-N*H*), 7.32–7.26 [m, 20H, Ar(*Bz*)], 7.11 (br, 4H, Ar*H*), 5.10 [m, 8H, OCH_2(Bz)], 4.67 and 4.31 (br, 4H and 4H, OCH_2CO), 3.90 and 3.45 (br, 4H and 4H, Gly-C$_\alpha H_2$), 3.2 and 4.51 (d, J = 14Hz, 4H and 4H, ArCH_2Ar), 2.10 (m, 4H, Val-C$_\alpha H$), 1.15–1.05 [br, 36H, Ar-C(CH_3)$_3$], 0.89, 0.88 [d, J = 6.5 Hz, 12H, 12H, Val-CH(CH_3)$_2$]. MALDI-TOF-MS (+ion, 2,5-didyroxybenzoic acid): Found, 1889.36 (Na^+), Calcd, 1889.32 (Na^+).

p-tert-*Butyl-calix[4]arene Tetra-val-gly-OH. p-tert*-Butyl-calix-[4]arene tetra-val-gly-OBz (0.1 g, 0.054 mmol) was added to a suspension of 10% Pd/C (0.01 g) in degassed methanol (20 ml). The mixture was stirred at room temperature under H_2 atmosphere for 8 h. The solution was filtered to remove the Pd/C and the filtrate evaporated to give a pure white solid (0.05 g, 63%). Electrospray ionization-MS (-ion, methanol/NEt_3): 1504.7; MALDI-TOF-MS (+ ion, 2,5-dihydroxybenzoic acid): Found, 1506.6 (H^+), Calcd: 1506.83 (H^+); Found, 1528.8 (Na^+); Calcd, 1528.82 (Na^+).

p-tert-*Butyl-calix[4]arene Tetra-valine-glycine-Tyrosine-Benzyl Ester* **3**. *N*-methylmorpholine (0.7 ml, 7 mmol) was added to a solution of tyrosine benzyl ester hydrochloride (1.352 g, 4.98 mmol) in dimethylformamide (0.4 ml). To this solution was then added *p-tert*-butyl-calix[4]arene tetra-val-gly-OH (0.25 g, 0.166 mmol) followed by *N*-hydroxybenzotriazole (HOBt) (0.68 g, 4.98 mmol). This mixture was stirred for 15 min, after which dicyclohexylcarbodiimide (1.02 g, 4.98 mmol) was added. The resulting mixture was protected from light and stirred at ambient temperature for 24 h. The solvent was evaporated on a rotary evaporator and the viscous material partially redissolved in CH_2Cl_2 (25 ml). The solution was filtered and the filtrate washed with 2 N HCl (aq) (15 ml), followed by 5% $NaHCO_3$ (aq) (2 × 10 ml). The organic layer was separated and solvent removed. The viscous pale yellow material was washed with acetone (40 ml) to give a white solid. This white solid was further purified by reversed-phase column chromatography by using C18 silica

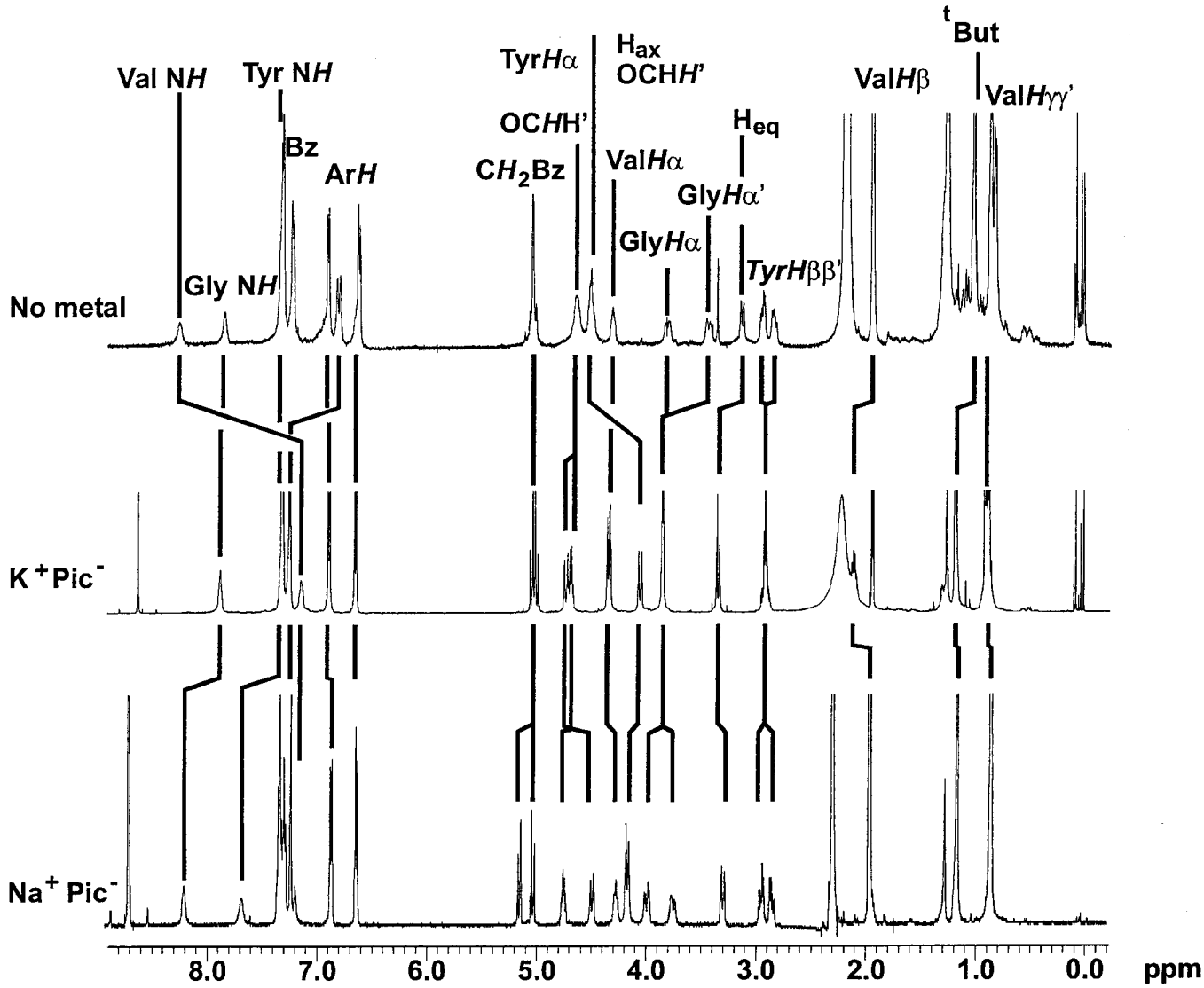

Fig. 2. ^{1}H NMR spectra (500 MHz, CD_3CN, 283 K) of **3** in the absence of metal ions (*Top*) or presence of K^+ picrate (*Middle*) presence of Na^+ picrate (*Bottom*).

eluting first with CH_3CN/H_2O (7:1) and then with 100% MeOH. ^{1}H NMR (CD_3CN, 500 MHz, 293 K), d 8.27 (br, 4H, Val-N*H*), 7.81 (br, 4H, Tyr-N*H*), 7.32–7.22 (m, Ar*H*), 7.11 (br, 4H, Gly-N*H*), 6.90 and 6.61 (d, J = 9Hz, 8H, 8H,Tyr-Ar*H*), 6.81 (d, 4H, Ar*H*), 5.04 (m, 8H, OCH_2(Bz)), 4.65 (d, J = 13 Hz, 4H, ArC*H*Ar), 4.51 (m, 4H, Tyr-$C_\alpha H$) 4.31 (d, 6.5Hz, 4H, Val-$C_\beta H$), 3.81 and 3.44 (dd, J = 15 Hz, 5.5 Hz, 4H, 4H, Gly-$C_\alpha H_2$), 3.13 (d, J = 13 Hz, 4H ArCH_2Ar), 2.95 and 2.84 (dd, J = 14 Hz, 6.5 Hz, 4H and 4H, Tyr-$C_\beta H_2$), 2.18 (m, J = 6.5 Hz, 4H, Val-$C_\alpha H$), 1.08 [s, 36H, Ar-C(CH_3)$_3$], 0.86 and 0.83 [d, J = 6.5 Hz, 12H, 12H, Val-($C_\gamma H_3$)$_2$]. MALDI-TOF-MS (+ion, 2, 5-dihydroxybenzoic acid): Found, 2542.01 (Na^+); Calcd, 2542.03 (Na^+); Found, 2558.22 (K^+), Calcd, 2558.14 (K^+).

Results

NMR and IR Metal-Binding Studies. Addition of Na^+ or K^+ ions[†] (15) to acetonitrile solutions of **1–3** altered the calixarene aromatic, methylene, *tert*-butyl, and OCH_2CO ^{1}H NMR resonances (Fig. 2 and Tables 1–9, and Figs. 5 and 7, which are published as supplemental data on the PNAS web site, www.pnas.org). These chemical shift changes indicate cation binding within the eight-oxygen pocket provided by the four -{OCH_2CO}- units appended to the calixarene framework. In addition, metal binding to **1-3** caused the four equivalent valine N—H resonances to be shifted upfield by 0.95–1.1 ppm. We assign such chemical shift changes to a structural rearrangement that involves replacement of N—H_{Val}···O═C hydrogen bonds by M^+···O═C bonds (M^+═Na^+ and K^+)[‡] (16). These amide proton resonances also exhibit an almost linear upfield shift on heating, a phenomenon characteristic of hydrogen bond breakage (Fig. 7, which is published as supplemental data on the PNAS web site, www.pnas.org) (17–20). Thus, in the absence of a metal ion, the valine amide protons of **1-3** are hydrogen bonded to carbonyls in the adjacent chains, forming a cyclic (..—NH···O═C—. . .)$_4$ network (Fig. 3). This interaction is not static and can be disrupted by molecular motions, explaining the observed upfield shifts on heat-

[†]Compounds **1-3** bind K^+ less well than Na^+ in acetonitrile. This difference is reflected in the more significant H^+ NMR chemical shift changes caused by Na^+ than by K^+ binding to **1-3**. The observed trend may be caused by the fact that Na^+ binds best to *p-tert*-butyl-calix[4]-(OCH_2COOR) (R = alkyl) (10). It must be noted, however, that metal-binding affinities in organic solvents and water may be reversed.

[‡]Switching of N—H···O═C hydrogen bonding with M$^+$···O═C binding interactions was proposed for **1** while the present study was in progress.

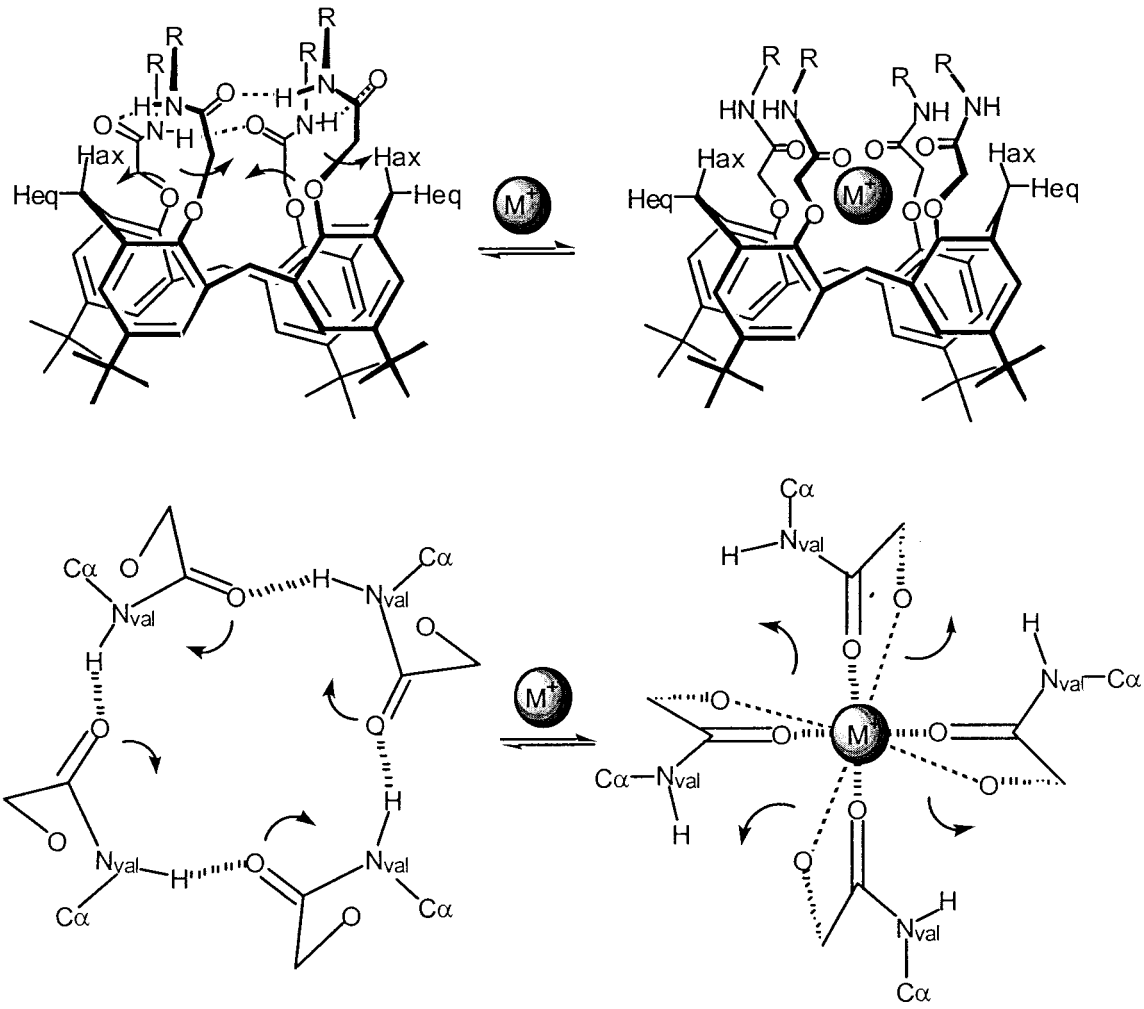

Fig. 3. Illustration of interchain N—H_{Val}···O═C hydrogen bonding by M^+···O═C-binding alternation in **1–3** [M^+ = Na^+ and K^+; *R* = $CH(CH(CH_3)_2)COCH_2Ph$ for **1**; *R* = $CH(CH(CH_3)_2)CONHCH_2COCH_2Ph$ for **2** and *R* = $CH(CH(CH_3)_2)CONHCH_2CONHCH(CH_2C_6H_5OH)COCH_2Ph$ for **3**]. *Upper*, side view. *Lower*, end view.

ing. Addition of the metal ion breaks the hydrogen bonds to the carbonyl oxygen atoms, also affording upfield-shifted amide proton resonances.

The structural rearrangements required for such H-bonding/M^+-binding switching are sensible as judged by examination of molecular models and seem to be facilitated by the flexibility of the -{OCH_2CO}- units. Thus, in **1–3,** N—H_{Val}···O═C hydrogen bonding and M^+···O═C binding (M^+ = Na^+ and K^+) are in equilibrium and compete with one another. Any weakening of the N—H_{Val}···O═C hydrogen bonds will favor M^+···O═C binding. We could estimate the approximate energetics of the hydrogen bonding contributions to this effect by examining the solid-state IR spectra of **1–3**. The compounds exhibit a broad $\nu_{N—H}$ band that shifts by 60–80 cm^{-1} to higher wavenumbers on addition of Na^+ or K^+ ions. This shift corresponds to a hydrogen bond energy of ≈2–3 kcal/mol (21). Thus interchain hydrogen bonds destabilize metal ion binding by ≈8–12 kcal/mol (see below).

Another important observation is that, in the absence of metal ions, the valine amide proton resonances appear at 7.67 ppm in **1**, at 7.98 ppm in **2,** and at 8.25 ppm in **3** (Fig. 7, www.pnas.org). We assign such downfield shifts to an increase in the valine N—H···O═C hydrogen bond strength arising from the formation of new interchain hydrogen bonding interactions further up the model filter in going from **1** to **3**. As a consequence, cation binding will be strongest in **1** and weakest in **3.** Correspondingly, cation release will be easier in **3** than in **2** and **1** (see below). In **2**, and even more so in **3**, the glycine amide proton resonances move downfield on addition of Na^+ ion and appreciably upfield on heating (Figs. 9 and 10, which are published as supplemental data on the PNAS web site, www.pnas.org). In **3,** the tyrosine amide resonances exhibit identical Na^+ and temperature dependencies. This result indicates that Na^+ promotes the involvement of the glycine amide in hydrogen-bonding interactions in **2** and **3** and of the tyrosine amide in **3,** probably because of motions triggered by the metal ion-induced H-bond breakage at the valine site.

Chemical shift changes in the ^1H NMR spectrum of **3** caused by addition of Na^+ ions occur not just in the calixarene-derived and valine amide proton resonances, as for **1** and **2**, but also in the rest of the VGY-OBz sequence (Figs. 2 and 4). Within the VGY-OBz units, the resonances shifting the most are the glycine C_α-H, followed by the tyrosine C_α-H and the $COOCH_2Ph$ protons at the C terminus. These chemical shift changes may indicate partial positive charge adjacent to these sites, as would occur by partial metal ion occupancy. This feature might be interpreted as the result of a doubly cation-populated calixarene molecule. This possibility would be allowed by the 5- to 10-fold metal excesses used in the metal-binding studies. MALDI and electrospray ionization MS, however, are consistent with the

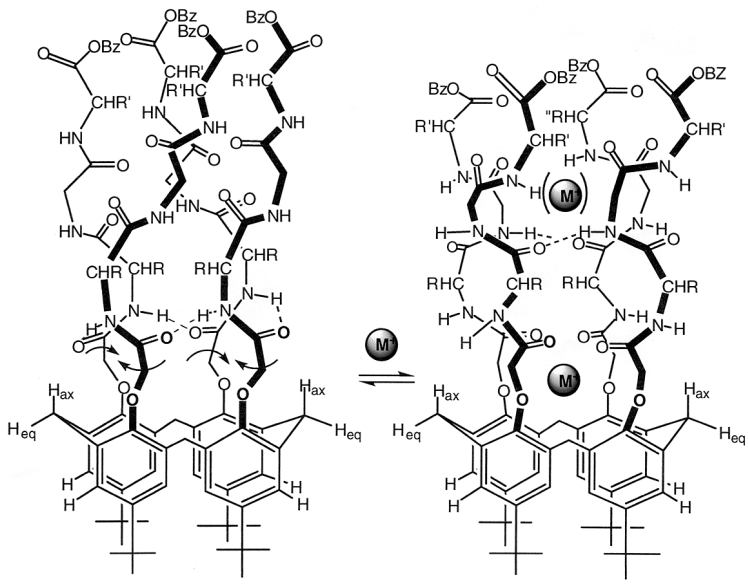

Fig. 4. Schematic representation of interchain hydrogen bonding and metal binding proposed for **3** on the basis of proton chemical shift changes [R = $CH(CH_3)_2$, R′ = CH_2-C_6H_4-OH]. The significant chemical shift changes observed up to the tyrosine amide proton suggest movement of the metal from the -{OCH_2CO}- to the glycine site (see text).

binding of only one cation. In addition, metal concentrations used were in the micro- to millimolar range, orders of magnitude lower than required for double ion occupancy in natural K^+ channels. Another possible explanation for the observed metal-induced ^1H NMR chemical shift changes in **3** is ion translocation along the $\{OCH_2CO\text{-}VGY\}_4$ unit. Considering that the stronger N—H···O═C H-bonding in **3** weakens ion binding, this hypothesis is reasonable and can be tested. Overall, the largest chemical shift changes in **3** match well the positions of a metal ion and a water molecule placement in the x-ray structure of the selectivity filter of KcsA (2). The metal ion is delocalized between T75- and V76-binding sites, and the water molecule binds at the G77 site.

Discussion

The present study demonstrates that a calix-[4]-arene framework affords a suitable template for the assembly of four peptide units to model features of the selectivity filter of the potassium channel. Two key findings are (*i*) that lengthening the polypeptide chains stabilizes interchain H-bonds between peptide amide functionalities and (*ii*) that metal binding competes with such hydrogen-bonding interactions.

Motions that permit the carbonyl oxygens to move toward or away from the pore can promote rapid binding and release of metal ions, respectively. This cation binding-release mechanism would have a low activation energy barrier if K^+-binding and H-bonding interactions compensated one another. We propose that such a mechanism may be operative in natural K^+ channels. The most likely site would appear to be G77, corresponding to the narrowest and most flexible point of the selectivity filter. The G77 amino acid is the only one for which an amide hydrogen bond partner has yet to be located in the current x-ray structure of KcsA. Interchain C···O contacts involving the glycines are extremely short. The distance between Cα of G77 and the O═C of G77 of the adjacent chain is ≈3.0 Å. If hydrogen atoms are placed in calculated positions, it is evident that a cyclic network of short C—H···O═C H-bonds (H···O ≈ 2 Å) can be formed. The same feature occurs at G79. It is possible that these hydrogen bonds occur in KcsA, although the distances may be too short. Small changes in the structure of the selectivity filter would allow G77 to participate in interchain N—H···O═C hydrogen bonding. Such motion within the selectivity filter could, as in our model compounds, allow interchain hydrogen bonding to occur at other positions.

The H-bonding/K^+-binding switching mechanism proposed here complements other proposals for explaining rapid ion movements in the channel, such as multiple ion occupancy. On the basis of the shape and dimensions of the pore and the steric requirements of the amino acid side chains, the strength of interchain N—H···O═C hydrogen bonding and K^+···O═C binding should differ along the TVGYG sequence. Motions within the selectivity filter may facilitate H-bonding/K^+-binding switching and could act as a thermodynamic driving force for ion translocation. The positive reinforcement of metal-binding and hydrogen-bonding interactions suggests an analogy to G-quartets, where such K^+-template effects leads to K^+ ion-binding selectivity (22–24). Ion translocation along K^+ channels has been recently investigated theoretically, suggesting that the most favorable conduction pathway requires a transition energy barrier of at most 5 kcal/mol (25). From an energetic point of view, even weak hydrogen bonds of ≈1–2 kcal/mol would be sufficient to lower the barrier (≈5–7 kcal/mol) significantly for ion translocation along the TVGYG sequence.

Conclusions

In summary, we report our initial attempt to model aspects of the KcsA potassium channel selectivity filter through synthetic modeling chemistry. We conclude that the first metal ion binds to the oxygen-rich environment formed by four -{OCH_2CO}- units, which resembles the T75-binding site of the natural channel. This result mimics the location of the metal ion partially situated at the T75- and V76-binding sites in the recent structure determination of KcsA (2). We find that, in the three model compounds, metal ion binding requires a cyclic network of interchain N—H···O═C hydrogen bonds involving the valine amide to be broken. We also observe that, by the cooperative effect of hydrogen bonding involving the glycine and tyrosine amides, interchain N—H_{Val}···O═C hydrogen bonds are stronger in **3,** which may facilitate ion release from the "T75-site." Given the flexibility that G77 provides to the selectivity filter, we propose such an ion-binding destabilization mechanism could also occur in natural channels, helping to lower the energy barrier for ion translocation.

Although the present work has afforded some new insights, it represents only a beginning. Important additional questions can be addressed by this approach. Included are understanding the chemical basis for K^+ selectivity, the maximum occupancy of

ions and water molecules in the TVGYG tetrapeptide filter sequence, the effect of mutations on the metal-binding and structural properties of the model filter, and the geometric conformations that can be adopted. The small size and solubility of the model compounds compared with the actual potassium channel are advantages in pursuing these objectives. The potential also exists for assembling lipid bilayers with embedded calix-[4]-arene tetrapeptide model filters to study ion transport properties.

We thank Profs. S. R. Tannenbaum [Massachusetts Institute of Technology (MIT)], L. J. Stern (MIT), and D. A. Kemp (MIT) for sharing instrumentation, and Prof. C. Miller (Brandeis University) for helpful comments on the manuscript. This work was supported by seed funds from MIT to S.J.L. to initiate research programs in neurochemistry.

1. Hille, B. (1992) *Ionic Channels of Excitable Membranes* (Sinauer, Sunderland, MA), pp. 1–19, 115–139.
2. Doyle, D. A., Cabral, J. M., Pfuetzner, R. A., Kuo, A., Gulbis, J. M., Cohen, S. L., Chait, B. T. & MacKinnon, R. (1998) *Science* **280,** 69–77.
3. Splitt, H., Meuser, D., Borovok, I., Betzler, M. & Schrempf, H. (2000) *FEBS Lett.* **472,** 83–87.
4. Hodgkin, A. L. & Keynes, R. D. (1955) *J. Physiol. (London)* **128,** 61–88.
5. Heginbotham, L. & MacKinnon, R. (1993) *Biophys. J.* **65,** 2089–2096.
6. Eisenman, G., Latorre, R. & Miller, C. (1986) *Biophys. J.* **50,** 1025–1034.
7. Vergara, C., Alvarez, O. & Latorre, R. (1999) *J. Gen. Physiol.* **114,** 365–376.
8. Yellen, G. (1998) *Quart. Rev. Biophys.* **31,** 239–295.
9. Miller, C. (2000) *Curr. Opin. Chem. Biol.* **4,** 148–151.
10. Arduini, A., Pochini, A., Reveberi, S. & Ungaro, R. (1986) *Tetrahedron Lett.* **42,** 2089–2100.
11. Gutsche, C. D. (1989) *Calixarenes* (Royal Society of Chemistry, Cambridge, U.K.).
12. Böhmer, V. (1995) *Angew. Chem. Int. Ed. Engl.* **34,** 713–745.
13. Ikeda, A. & Shinkai, S. (1997) *Chem. Rev.* **97,** 1713–1734.
14. Ungaro, R., Pochini, A. & Andreetti, G. D. (1984) *J. Inclusion Phenom.* **2,** 199–206.
15. Prestegard, J. H. & Chan, S. I. (1970) *J. Am. Chem. Soc.* **92**, 4440–4446.
16. Nomura, E., Takagaki, M., Nakaoka, C., Uchida, M. & Taniguchi, H. (1999) *J. Org. Chem.* **64,** 3151–3156.
17. Golubev, N. S., Denisov, G. S., Smirnov, S. N., Shchepkin, D. N. & Limbach, H. H. (1996) *Z. Phys. Chem. (Munich)* **196,** 73–84.
18. Raj, P. A., Soni, S. D., Ramasubbu, N., Bhandary, K. K. & Levine, M. J. (1990) *Biopolymers* **30,** 73–85.
19. Ng, S. (1980) *Spectrochim. Acta A* **36,** 927–928.
20. Sleijko, F. L., Drago, R. S. & Brown, D. G. (1972) *J. Am. Chem. Soc.* **94,** 9210–9216.
21. Iogansen, A. V., Kurkchi, G. A., Furman, V. M., Glazunov, V. P. & Odinokov, S. E. (1980) *Zh. Prikl. Spektrosk.* **33,** 460–466.
22. Bouaziz, S., Kettani, A. & Patel, D. J. (1998) *J. Mol. Biol.* **282,** 637–652.
23. Hud, N. V., Schultze, P., Sklenár, V. & Feigon, J. (1999) *J. Mol. Biol.* **285,** 233–243.
24. Basu, S., Rambo, R. P., Strauss-Soukup, J., Cate, J. H., Ferré-D'Amaré, A. R., Strobel, S. A. & Doudna, J. A. (1998) *Nat. Struct. Biol.* **5,** 986–992.
25. Åqvist, J. & Luzhkov, V. (2000) *Nature (London)* **404,** 881–884.